Published in final edited form as:
*J Immunol*. 2006 January 15; 176(2): 790–802.

# Early Preplasma Cells Define a Tolerance Checkpoint for Autoreactive B Cells[1]

**Donna A. Culton**, **Brian P. O'Conner**, **Kara L. Conway**, **Ramiro Diz**, **Jennifer Rutan**, **Barbara J. Vilen**, and **Stephen H. Clarke**[2]
Department of Microbiology and Immunology, University of North Carolina, Chapel Hill, NC 27599

## Abstract

Ab-secreting plasma cells (PCs) are the effectors of humoral immunity. In this study, we describe regulation of autoreactive B cells specific for the ribonucleoprotein Smith (Sm) at an early pre-PC stage. These cells are defined by the expression of the PC marker CD138 and normal levels of CD19 and B220. They are present at a high frequency in normal mouse spleen and bone marrow, are Ag dependent, and are located predominantly along the T cell-B cell border and near bridging channels. Anti-Sm pre-PCs also occur at a high frequency in nonautoimmune mice and show additional phenotypic characteristics of PC differentiation. However, while some of these pre-PCs are Ab-secreting cells, those specific for Sm are not, indicating regulation. Consistent with this, anti-Sm pre-PCs have a higher turnover rate and higher frequency of cell death than those that do not bind Sm. Regulation of anti-Sm pre-PCs occurs upstream of the transcriptional repressor, B lymphocyte-induced maturation protein-1, expression. Regulation at this stage is overcome in autoimmune MRL/*lpr* mice and is accompanied by an altered B lymphocyte stimulator receptor profile. These data reveal a new B cell tolerance checkpoint that is overcome in autoimmunity.

Humoral immune responses to foreign Ag involve differentiation of mature B cells to Ab-secreting cells (ASCs)[3] or plasma cells (PCs) (1). Responses to both T-independent (TI) and T-dependent (TD) Ags result in the formation of short-lived PCs and TD Ags give rise to long-lived PCs that derive from germinal centers (2, 3). Numerous changes are associated with PC differentiation, including the loss of surface IgM, CD19, and MHC class II, the production of secretory IgM, and the up-regulation of the PC marker CD138 (syndecan-1) (1). Recently, PCs have been found to up-regulate the B lymphocyte stimulator (BlyS) receptor, B cell maturation Ag (BCMA), and chemokine receptor CXCR4, which are necessary for PC survival and homing to the bone marrow (BM), respectively (4-11).

PC differentiation is largely controlled by the transcriptional repressor B lymphocyte-induced maturation protein-1 (Blimp-1) (12). Direct targets of Blimp-1 repression are c-

[1]This work was supported by National Institutes of Health Grants AI29576 and AI43587 and Training Grant in Dermatological Research T32 AR07369.



[2]Address correspondence and reprint requests to Dr. Stephen H. Clarke, Department of Microbiology and Immunology, CB No. 7290 804 Mary Ellen Jones Building, University of North Carolina, Chapel Hill, NC 27599. shl@med.unc.edu.

**Disclosures**
The authors have no financial conflict of interest.

[3]Abbreviations used in this paper: ASC, Ab-secreting cell; PC, plasma cell; TI, T independent; TD, T dependent; BlyS, B lymphocyte stimulator; BCMA, B cell maturation Ag; BM, bone marrow; Blimp-1, B lymphocyte-induced maturation protein-1; XBP-1, X box-binding protein 1; Sm, Smith; SLE, systemic lupus erythematosus; Tg, transgenic; FO, follicular; MZ, marginal zone; CT, cycle threshold; HEL, hen egg lysozyme; PNA, peanut agglutinin; DC, dendritic cell; PALS, periarteriolar lymphoid sheath; IC IgM, intracellular IgM; BAFF-R, B cell-activating factor receptor; TACI, transmembrane and calcium modulator and cyclophilin ligand; APRIL, a proliferation-inducing ligand; int, intermediate.

*myc*, Pax5 (encoding B cell-specific activator protein), MHC CIITA, SpiB, and Id3 (12, 13). Blimp-1 is also important for induction of X box-binding protein 1 (XBP-1), the only other transcription factor required for PC differentiation (14, 15). Thus, Blimp-1 plays a critical role in PC differentiation by inducing cell cycle arrest, induction of Ig secretion, and inhibition of germinal center function (12).

The cellular differentiation of B cells to PCs has not been completely elucidated, but recently several intermediate stages of PC differentiation have been described (6, 7, 14, 16-18). These intermediates differ in function and phenotype exhibiting characteristics of mature B cells and PCs ($B220^{low}$, $CD19^{+}$, surface $Ig^{low}$, $CD138^{+}$, high intracellular $Ig^{+}$, and Ig secretion). It is not clear how the different intermediates relate to one another and whether they all exist on a single differentiative pathway.

Multiple mechanisms of B cell regulation, including central deletion, receptor editing, peripheral deletion, and anergy (19-28), block anti-self B cell differentiation to ASCs thereby preventing autoimmunity. Several of these mechanisms regulate B cells specific for Smith (Sm), a ribonucleoprotein uniquely targeted in systemic lupus erythematosus (SLE). In transgenic (Tg) mice that posses an anti-Sm H chain rearrangement (2-12H), anti-Sm B cells comprise 30–50% of peripheral B cells and are present as transitional, follicular (FO), and marginal zone (MZ) B cells in the spleen and as B-1 cells in the peritoneum (29, 30). Despite the large number of anti-Sm B cells, serum anti-Sm in 2-12H Tg mice is no different from non-Tg mice indicating that tolerance is maintained and PC differentiation prohibited (29). Anti-Sm B cells are regulated by developmental arrest, anergy, and ignorance after differentiation to MZ and B-1 B cells (29-32). In this study, we describe a new regulatory checkpoint that occurs after activation at an early pre-PC stage. Regulation of autoreactive B cells at a pre-PC stage prompts new considerations regarding the fundamentals of B cell activation and early PC differentiation in the context of autoimmunity and tolerance.

## Materials and Methods

### Mice

2-12H Tg, 2-12H Tg MRL/*lpr*, MD4 and MD4 × ML5 mice have been previously described (24, 29, 33) and were housed and bred in a conventional facility at the University of North Carolina (Chapel Hill, NC). Screening of 2-12H mice for the transgene was performed by PCR analysis of tail genomic DNA as previously described (29). All mice were 2–8 mo of age at the time of analysis. MD4 and MD4 × ML5 mice were the gift of P. Oliver (National Jewish Medical and Research Center, Denver, CO) and K. Hippen (University of Minnesota Medical School, Minneapolis, MN).

### Flow cytometry

Single-cell suspensions of splenocytes were prepared and RBCs were lysed using an RBC lysis solution (1 M Tris, 0.15 M ammonium chloride, and 0.1 M EDTA). All staining was done in RPMI 1640 medium (HyClone) containing 3.0% bovine calf serum (HyClone) as described (30). FcRs were blocked with mAb 2.4G2 for 20 min at 4°C. Cells were analyzed at the University of North Carolina Flow Cytometry Facility (Chapel Hill, NC) using a FACSCalibur (BD Biosciences). The Abs specific for CD19 (1D3), CD138 (281-2), IgM (II/41), B220 (RA3-6B2), CD21 (7G6), CD23 (B3B4), CD80 (16-10A1), CXCR4 (2B11), and CXCR5 (2G8) were obtained from BD Pharmingen and were labeled with FITC, PE, allophycocyanin, biotin, or Alexa 647. For the detection of apoptotic cells, CaspACE FITC-VAD-FMK was used as described by the manufacturer (Promega). For the identification of anti-Sm B cells, we used Sm (SMA-3000; Immunovision) that was biotinylated in our laboratory as described previously (29). For the detection of biotinylated probes we used

streptavidin-FITC, streptavidin-PerCP (BD Pharmingen), or streptavidin-allophycocyanin (BD Pharmingen). Data were analyzed using Summit software (Dako-Cytomation). All data represent cells that fell within the lymphocyte gate determined by forward and 90° light scatter. One to $5 \times 10^5$ cells per sample were analyzed. All contour plots are 5% probability.

### Immunohistochemistry

Freshly isolated spleens were embedded in Tissue-Tek OCT (Sakura Finetek) and frozen in 2-methyl-butane and liquid nitrogen. Six-micrometer spleen sections were prepared and fixed for 5 min in acetone:MeOH at −20°C before staining. Sections were blocked for 1 h with Superblock Blocking buffer in PBS (1:1 ratio) containing 2.4G2 anti-Fc$\gamma$R Ab. Slides were rinsed and stained at room temperature for 2 h with anti-CD138-PE, IgM-Alexa 350 (Molecular Probes), anti-CD3-allophycocyanin (BD Pharmingen), anti-CD11b-biotin, and anti-CD11c-biotin (eBioscience) diluted in blocking buffer. CD11b and CD11c staining was revealed by streptavidin Alexa 488 (Molecular Probes). Stained slides were rinsed with PBS and coverslips mounted in FluorSave mounting media (Calbiochem). Analysis was performed using a digital deconvolusion microscope (Intelligent Imaging Innovations (3I)). Images were collected and analyzed using Slidebook software (3I).

### IC IgM detection

Cell surface proteins were stained as described above. During the staining of cell surface proteins, surface Ig was blocked using unlabeled anti-IgM (II/41; BD Pharmingen) at 2 $\mu$g/$10^6$ cells for 20 min at 4°C. After washing with RPMI 1640, cells were washed once with PBS and fixed with 1% paraformaldehyde in PBS (200 $\mu$l/$10^6$ cells for 10 min at 4°C). After fixation, cells were permeabilized with saponin buffer (0.05% in PBS containing 0.5% BSA) using 100 $\mu$l/$10^6$ cells for 30 min at 4°C. Cells were then stained with anti-IgM-FITC (II/41; BD Pharmingen) in saponin buffer using 50 $\mu$l/$10^6$ cells at a previously determined optimal concentration for 30 min at 4°C. Cells were washed twice with saponin buffer and once with RPMI 1640 before analysis in RPMI 1640 as described above.

### Cell sorting

For cell-sorting experiments, spleen cells were stained with Ab as described for each experiment and sorted on a MoFlo high-speed sorter (DakoCytomation). Sorted populations were >90% pure as determined by reanalysis.

### Ex vivo ELISPOT

ELISPOT was performed as previously described (30) using ImmunoSpot Mid Plates (Cellular Technology) were coated with 10 U/well Sm Ag (Immunovision), anti-IgM (Southern Biotechnology Associates), or anti-Ig (Southern Biotechnology Associates). Sorted cells were resuspended in HL-1 medium (BioWhittaker) supplemented with 1% L-glutamine and 1% penicillin/streptomycin; ~$1 \times 10^5$ cells were added to each well and 1/2 serial dilutions were made across the plate. Spots were detected using biotin-labeled anti-$IgM^a$ or $IgM^b$ Ab (BD Pharmingen), streptavidin-HRP (BD Pharmingen), or anti-IgG HRP (Southern Biotechnology Associates) and developed with 3-amino-9-ethylcarbazole (Sigma-Aldrich) in 3-amino-9-ethylcarbazole buffer. The plates were scanned and analyzed using an ELISPOT Analyzer (Cellular Technology).

### BrdU incorporation

Mice were given 0.5 mg/ml BrdU (Sigma-Aldrich) with 1 mg/ml dextrose in their drinking water continuously for 1 wk and spleens cells were prepared for flow cytometry as described above. Staining for BrdU was done as described by Allman et al. (34) using anti-BrdU-FITC (BD Biosciences).

### Cell cycle analysis

Cells were stained with CD19-allophycocyanin, CD138-PE, and Sm and were sorted as described above. The cells were then fixed with 70% ethanol and stained with a buffer containing 100 μg/ml propidium iodide and 250 μg/ml RNase A (Boehringer Mannheim) overnight at 4°C. The DNA content was analyzed by FACSCalibur, as described above.

### Real time RT-PCR

$CD138^{-}$, $CD138^{int}$, and $CD138^{high}$ $CD19^{+}$ B cells were positively selected to a purity of >90% via FACS sorting using Ab combinations against 2-12Tg BCR, CD138, and CD19. Total RNA was isolated from the purified cell samples by the TRIzol method (Invitrogen Life Technologies) followed by a DNase-I treatment step. One microgram of DNA-free RNA was reverse-transcribed to cDNA using Moloney murine leukemia virus reverse transcriptase (Invitrogen Life Technologies). Real-time PCR was performed with the Absolute SYBR Green Mix (ABgene) on an ABI Prism 7900HT sequence detection system (Applied Biosystems). Amplification conditions were as follows: 50°C for 2 min, 95°C for 15 min, followed by 40 cycles of 95°C for 15 s, 56°C for 30 s, and 72°C for 15 s. Real-time primers were designed using Primer3 software, with a specified amplicon length between 100 and 250 bp. Primers for the control gene mouse β-actin were as follows: forward, 5′-AGGGCTATGCTCTCCCTCAC-3′ and reverse, 5′-CTCTCAGCTGTGGTGGTGAA-3′. Other primers used were as follows: BCMA, forward, 5′-ATCTTCTTGGGGCTGACCTT-3′ and reverse, 5′-CTTTGAGGCTGGTCCTTCAG-3′; B cell-activating factor receptor (BAFF-R), forward, 5′-CCCCAGACACTTCAGAAGGA-3′ and reverse, 5′-AGGTAGGAGCTGAGGCATGA-3′; transmembrane activator and calcium modulator and cyclophilin ligand interactor (TACI), forward, 5′-GTGTGGCCACTTCTGTGAGA-3′ and reverse, 5′-CTGGTGCCTTCCTGAGTTGT-3′; Blimp-1, forward, 5′-TGTTGGATCTTCTCTTGGAAAA-3′ and reverse, 5′-GTGTAAAGTAGACTGCCTTGA 3′; CD138, forward, 5′-CTCACTAGGCTCCCACTTGC-3′ and reverse 5′-ATGCAAGAAACCCTTTGCAC-3′. Relative expression of RNA was determined via: relative expression = $2^{-(\Delta\Delta CT)} \times 1000$, where ΔΔCT = (cycle threshold (CT) gene of interest) – (CT β-actin in experimental sample) – (CT gene of interest – CT β-actin in a no-template control sample). Statistical *p* values were determined via a two-tailed paired *t* test. Real-time SYBR-green dissociation curves show one species of amplicon for each primer combination (data not shown). Agarose gels (1.5%) show a single PCR product of the appropriate size (data not shown).

### Statistical analysis

The paired Student's *t* test and the independent Student's *t* test were used to assess the significance of the observed differences. A value of $p < 0.05$ was considered significant.

## Results

### Anti-Sm B cells are present at a $CD138^{int}$ B cell stage

We have previously shown that immunization of 2-12H mice with apoptotic cells or small nuclear ribonucleoproteins induces an anti-Sm response and anti-Sm B cells are activated upon transfer to mice deficient in clearance of apoptotic cells (29, 30). To understand the activation of anti-Sm B cells, we looked for the presence of pre-PCs and PCs in the spleens of 2-12H and 2-12H MRL/*lpr* mice using CD138 as a marker (1, 5-7, 14, 16-18). Few $CD19^{-/low}$, $CD138^{+}$ PCs were present in the spleens of non-Tg and 2-12H mice. However, a population of B cells expressing intermediate levels of CD138 ($CD138^{int}$), and normal levels of CD19 and B220, was observed (Fig. 1*A*, and data not shown). They are distinct from pre-PCs described previously that have high levels of CD138 and low levels of CD19

and B220 (6, 7, 14, 18). The CD138$^{int}$ B cells comprise ~20% of the anti-Sm CD19$^{+}$ cells in 2-12H mice and ~20% of non-Sm binding B cells from 2-12H and non-Tg mice (Fig. 1*B*). Most were CD23$^{+}$ and CD21$^{int}$ similar to FO B cells, although a small subset were CD23$^{low}$ and CD21$^{high}$ similar to MZ B cells (Fig. 1*C*). Thus, a large fraction of normal mouse B cells express the PC marker CD138. Interestingly, autoreactive B cells are enriched in the CD138$^{int}$ population of non-Tg mice; ~20% and ~13% CD138$^{int}$ and CD138$^{-}$ non-Tg B cells, respectively, were anti-Sm, a nearly 2-fold enrichment in the CD138$^{int}$ population (Fig. 1*D* and Table I). Thus, autoreactive B cells of normal mice are enriched in the CD138$^{int}$ population and a substantial fraction of CD138$^{int}$ cells are autoreactive.

CD138$^{int}$ B cells were also present in the BM (Fig. 1, *E* and *F*). Twenty-five to 30% of mature (IgD$^{+}$ and/or CD23$^{+}$) B cells were CD138$^{int}$, and in 2-12H mice this population included anti-Sm B cells. Thus, significant numbers of CD138$^{int}$ B cells are present in the BM and spleen.

To determine whether Ag stimulation is required for anti-Sm CD138$^{int}$ B cell differentiation, we compared the expression levels of activation markers on CD138$^{-}$ and CD138$^{int}$ B cells. Both flow cytometry and light microscopy of Wright-Giemsa-stained cells indicated that the CD138$^{int}$ or CD138$^{-}$ B cells of non-Tg did not differ in size or granularity (Fig. 1*C*, *first column*, and data not shown). However, the anti-Sm CD138$^{int}$ B cells from 2-12H mice were significantly larger and more granular by flow cytometry, and had significantly lower surface IgM levels than CD138$^{-}$ B cells (Fig. 1*C*). In addition, chemokine receptor expression levels were different; CXCR4 was significantly increased and CXCR5 was significantly decreased on anti-Sm CD138$^{int}$ compared with CD138$^{-}$ B cells (Fig. 1*C*). The differences in CD80 expression were not significant, although the pattern of expression was different (Fig. 1*C*). In contrast to the phenotypic differences between anti-Sm CD138$^{-}$ and CD138$^{int}$ B cells of 2-12H mice, CD138$^{-}$ and CD138$^{int}$ B cells of non-Tg mice differed only in IgM and CXCR5 expression levels (Fig. 1*C*). No differences were seen in CD86, MHC class II, peanut agglutinin (PNA), and GL7 expression between CD138$^{-}$ and CD138$^{int}$ B cells from mice of either strain (data not shown). Thus, the differences between the anti-Sm CD138$^{-}$ and CD138$^{int}$ B cells of 2-12H mice suggest that the latter have encountered Ag, consistent with a model in which they have begun PC differentiation.

To more definitively address the requirement for Ag, we determined whether Ag was required for the development of CD138$^{int}$ B cells specific for hen egg lysozyme (HEL). As shown in Fig. 1, *B* and *G*, there was a significantly ($p = 0.0002$) higher frequency of anti-HEL CD138$^{int}$ B cells in the presence of Ag (~10%; MD4 × ML5 mice) than in the absence of Ag (MD4 only mice; ~0.70%). CD138 staining is unlikely to be artifactual; real-time PCR shows that CD138 mRNA expression was higher in sorted CD138$^{int}$ cells than CD138$^{-}$ cells (Fig. 1*E*), and the CD138$^{int}$ B cells were significantly larger and more granular ($p < 0.01$) than CD138$^{-}$ B cells (Fig. 1*E*). Anti-HEL B cells were transitional, FO, and MZ in similar proportions in the presence or absence of HEL (data not shown) indicating that changes in subset distribution caused by the presence of Ag cannot explain the increase in CD138$^{int}$ B cell frequency. To assess whether a BCR signal is similarly required for CD138$^{int}$ B cell differentiation in non-Tg mice, we generated mice with low levels of CD19 (CD19$^{+/-}$), a positive regulator of BCR signaling. As shown in Fig. 1*B*, there was a significant decrease in the frequency of CD138$^{int}$ B cells suggesting the requirement for a BCR signal. Thus, CD138$^{int}$ B cell differentiation is Ag dependent, and self-Ag can induce autoreactive B cells to differentiate to the CD138$^{int}$ stage in nonautoimmune mice.

### Pre-PCs are located in follicles primarily near bridging channels and the T cell areas

Activated B cells typically migrate within follicles (9) and we therefore determined the location of CD138$^{int}$ B cells in the spleen by immunohistochemistry. Because multiple cell types express CD138, sections were stained for CD138 and for CD3, CD11b, CD11c, and IgM to discriminate B cells from T cells, macrophages, and dendritic cells (DCs). In non-Tg and 2-12H mice, CD138$^{int}$ B cells were located primarily in follicles (Fig. 2, *A* and *B*), and were rare in the MZ and red pulp. Within the follicle, the CD138$^{int}$ B cells were generally clustered, and were more likely to be found near the border with the T cell-rich periarteriolar lymphoid sheath (PALS) and bridging channels. In addition, the CD138$^{int}$ B cells proximal to the PALS border and bridging channels tended to stain more intensely for CD138 than those located more distally. Location in these areas allowed for proximity of some CD138$^{int}$ B cells to T cells and DCs. These data suggest that CD138$^{int}$ B cells migrate toward the T cell region and bridging channels. This is similar to migration induced by TI Ags (35).

### Anti-Sm B cells are regulated at the CD138$^{int}$ B cell stage

To further test the possibility that CD138$^{int}$ B cells were pre-PCs, they were examined for intracellular IgM (IC IgM) and Ab secretion (6, 16, 17). In both 2-12H and non-Tg mice a higher frequency of CD138$^{int}$ than CD138$^{-}$ B cells were IC IgM$^{high}$ (Fig. 3, *A* and *B*) suggestive of PC differentiation. Moreover, a higher frequency of CD138$^{int}$ than CD138$^{-}$ B cells of non-Tg mice secreted Ab (IgM or IgG) according to an ELISPOT assay (Fig. 3*C*). Although CD138$^{int}$ B cells constitute a minority of the B cell population, they contribute 8-fold more IgM and IgG ASCs than CD138$^{-}$ B cells (Table II). Similarly, a higher frequency of CD138$^{int}$ than CD138$^{-}$ B cells of 2-12H mice were ASCs, although the difference was considerably smaller than in non-Tg mice. The frequency of IgM ASCs from non-Tg and 2-12H mice was low among CD138$^{int}$ B cells (<1%) (Fig. 3*C*), but this is consistent with the low frequency IC IgM$^{high}$ B cells (<3%) (Fig. 3*B*) and with their early pre-PC phenotype. Most significantly, there was no difference between 2-12H CD138$^{int}$ and CD138$^{-}$ B cells in the frequency of anti-Sm-secreting cells (Fig. 3*C* and Table II). There was also no difference in the number anti-HEL CD138$^{-}$ and CD138$^{int}$ ASCs from anti-HEL mice (data not shown). Because anti-Sm ASCs were largely absent, we presumed that the IgM ASCs among CD138$^{int}$ B cells of 2-12H mice had either a low affinity for Sm or did not bind Sm. The low frequency of IgM ASCs from 2-12H mice is seemingly at odds with the high frequency of splenic B cells falling outside of the Sm-binding gate (Fig. 1*A*). However, many 2-12H B cells show weak staining with Sm (Fig. 1*A*) and are likely to have low affinity anti-Sm BCRs. As a result, they too may be subject to regulation resulting in the low frequency of IgM ASCs observed. Thus, while some non-Sm CD138$^{int}$ B cells had become ASCs, consistent with their early pre-PC phenotype, the autoreactive anti-Sm and anti-HEL CD138$^{int}$ B cells had not.

### Anti-Sm CD138$^{int}$ B cells are not regulated in autoimmune 2-12H Tg MRL/lpr mice

To determine how anti-Sm CD138$^{int}$ B cells were regulated differently in autoimmune mice, we examined 2-12H MRL/*lpr* mice. Both Sm binding and non-Sm binding CD138$^{int}$ B cells were present in the spleens of 2-12H MRL/*lpr* mice (Fig. 4, *A* and *B*), but they were present at a lower frequency than in nonautoimmune mice (Fig. 1, *A* and *B*). As with nonautoimmune mice, a large fraction of CD138$^{int}$ B cells from non-Tg MRL/*lpr* mice were anti-Sm (Fig. 4*C*), and the anti-Sm B cells were enriched (~3-fold) in this population relative to the CD138$^{-}$ population (~35 vs ~11%; Fig. 4*C* and Table I). Compared with CD138$^{-}$ B cells, anti-Sm CD138$^{int}$ B cells had lower IgM levels, increased CXCR4, and decreased CXCR5 levels, and most had high levels of CD80 (Fig. 4*D*). These expression differences were more pronounced than those in nonautoimmune mice (compare Fig. 4*D* with 1*C*). There was no difference in PNA or GL-7 expression (data not shown). Similar results were observed with non-Sm binding CD138$^{-}$ and CD138$^{int}$ B cells (data not shown).

As in nonautoimmune mice, some CD138$^{int}$ B cells were IC IgM$^{high}$ and ASCs, but the frequencies in both MRL/*lpr* and 2-12H MRL/*lpr* mice (IC IgM$^{high}$: 10–30%; ASCs: 1.5–2.0%) were higher than in their nonautoimmune counterparts (IC IgM$^{high}$: 2–3%, ASCs: <1%) (Fig. 4, *E* and *F*). Most significantly, the frequency of anti-Sm ASCs among CD138$^{int}$ B cells of 2-12H MRL/*lpr* mice was higher than among anti-Sm CD138$^{-}$ B cells ($p < 0.05$; Fig. 4*F*). The average number of anti-Sm ASCs among CD138$^{int}$ from 2-12 MRL/*lpr* was 4129 ± 1557 per $10^6$ B cells (range: 0–12,687/$10^6$; $n = 11$; Fig. 4*F*), but was 155 ± 54 per $10^6$ B cells in 2-12H mice (range: 0–196; $n = 8$; $p = 0.045$; Fig. 4*C*). Thus, the anti-Sm CD138$^{int}$ cells of MRL/*lpr* mice showed a more activated and differentiated phenotype than those of nonautoimmune mice, with a higher frequency having become ASCs.

Anti-Sm B cells of MRL/*lpr* mice had also differentiated to a CD138$^{high}$ stage in both MRL/*lpr* and 2-12H MRL/*lpr* mice. These cells were also CD19$^{low}$ and B220$^{low}$ (Fig. 4, *A* and *B*, and data not shown), and in 2-12H MRL/*lpr* mice this population included anti-Sm B cells (Fig. 4, *A* and *B*). Their frequency was significantly higher in 2-12H MRL/*lpr* mice than in 2-12H mice where they were barely detectable (0.66 ± 0.13% and 0.13 ± 0.025%, respectively; $p = 0.0084$; see legend to Fig. 4*A*). Their phenotype resembled that of the late pre-PCs described previously (6, 14). Consistent with a later stage of differentiation, the anti-Sm CD138$^{-}$ and CD138$^{high}$ B cells were generally more different in the expression levels of IgM, CD80, CXCR4, and CXCR5 than were anti-Sm CD138$^{-}$ and CD138$^{int}$ B cells, although not all differences were statistically significant, owing in part to greater heterogeneity in expression levels between mice (Fig. 4*D*). CD138$^{high}$ B cells did not show increased expression of either PNA or GL-7. A higher proportion of CD138$^{high}$ than CD138$^{int}$ B cells were IC IgM$^{high}$ and ASCs (Fig. 4, *E* and *F*). The frequency of anti-Sm ASCs among CD138$^{high}$ B cells was also higher than among CD138$^{-}$ B cells (Fig. 4, *E* and *F*). This frequency is lower than the frequency of IgM ASCs consistent with the fact that not all B cells are anti-Sm. The CD138$^{int}$ and CD138$^{high}$ B cells contributed 10–20 times the number of IgM and IgG ASCs, and 3 times the number of anti-Sm ASCs, as CD138$^{-}$ B cells (Table II). Based on a postsort analysis, <1% of the CD138$^{int}$ ASCs could be attributed to contaminating CD138$^{high}$ B cells and even fewer could be due to contaminating CD138$^{+}$CD19$^{-}$ PCs (data not shown). Thus, anti-Sm CD138$^{int}$ pre-PCs of MRL/*lpr* mice differentiated to CD138$^{high}$ pre-PCs and PCs.

Immunohistochemistry analysis indicated that the distribution of CD138$^{+}$ B cells in MRL/*lpr* is similar to that in nonautoimmune mice. However, there are significant architectural differences in the white pulp of MRL/*lpr* mice compared with nonautoimmune mice. A MZ region rich in B cells surrounded the follicle and PALS (Fig. 2, *C* and *D*). B cells were also located in a follicle that is often separated from the MZ by an infiltration of T cells into the marginal sinus (Fig. 2, *C* and *D*). Staining with PNA did not reveal germinal centers (data not shown). Despite these differences, as in nonautoimmune mice, CD138$^{+}$ B cells were located primarily in the follicle and were rare in the encircling MZ and in the red pulp. In the follicles, B cells staining brightly and weakly for CD138 were evident, consistent with the flow cytometry analysis. Thus, the CD138$^{+}$ B cells of MRL/*lpr* mice are located primarily in follicles.

### Anti-Sm CD138$^{int}$ B cells progress toward apoptosis

To understand the regulation of anti-Sm CD138$^{int}$ B cells in non-autoimmune mice, we examined cell cycle, half-life, and cell death. The absence of anti-Sm ASCs among CD138$^{int}$ B cells of 2-12H Tg mice could be due to their elimination before becoming competent to secrete Ab. A BrdU incorporation assay indicated that anti-Sm CD138$^{int}$ B cells of nonautoimmune mice incorporated BrdU more rapidly than nonautoreactive CD138$^{int}$ B cells (Fig. 5*A*). Moreover, few anti-Sm and non-Sm CD138$^{int}$ B cells were in cycle (Fig. 5*B*). Cell division was unlikely to occur before expression of CD138 because

<1% of CD138$^-$ B cells were in cycle (data not shown). Thus, in the absence of proliferation of anti-Sm CD138$^-$ and CD138$^{int}$ B cells, the BrdU incorporation rate would reflect the 50% turnover rate of the cells, estimated to be ~7 days for anti-Sm CD138$^{int}$ B cells and ~21 days for non-Sm binding CD138$^{int}$ B cells from nonautoimmune mice. Consistent with this difference in turnover rate, a high frequency (~17%) of anti-Sm CD138$^{int}$ B cells were undergoing apoptosis, based on staining with the caspase inhibitor VAD-FMK (Fig. 5*C*). In contrast, only ~4% of non-Sm CD138$^{int}$ B cells were apoptotic. Some anti-Sm CD138$^-$ B cells may be eliminated before they reach the CD138$^{int}$ stage, because a high frequency of these cells were VAD-FMK$^+$ (~12%) (Fig. 5*C*). These data indicate that anti-Sm CD38$^{int}$ B cells of nonautoimmune mice do not enter cell cycle and have a rapid turnover rate at least partly due to cell death, while the non-Sm CD138$^{int}$ B cells also do not enter cell cycle but have a relatively long turnover rate.

An analysis of anti-Sm CD138$^{int}$ B cells of MRL/*lpr* mice showed evidence of both entry into cell cycle and apoptosis. The anti-Sm CD138$^{int}$ B cells of MRL/*lpr* mice had a comparable BrdU incorporation rate to those in nonautoimmune mice (Fig. 5*A*). This rate was similar to those of their non-Sm binding counterparts (Fig. 5*A*). This high incorporation rate for anti-Sm CD138$^{int}$ B cells was likely due to cell division in the spleen, because ~3% of anti-Sm and ~7% of non-Sm CD138$^{int}$ B cells were in cycle (Fig. 5*B*). This proliferation precluded an estimation of half-life. Also, a high frequency of anti-Sm CD138$^{int}$ B cells in 2-12H MRL/*lpr* was VAD-FMK$^+$ (~22%). Thus, some anti-Sm B cells undergo apoptosis after they reach the CD138$^{int}$ stage (Fig. 5*C*), as they do in nonautoimmune mice, while others must continue differentiation to the CD138$^{high}$ and PC stages.

## Autoreactive CD138$^{int}$ B cell regulation and Blimp-1 transcription

To understand the molecular basis of CD138$^{int}$ B cell regulation, we examined Blimp-1 mRNA expression by real-time PCR. Blimp-1 mRNA levels were significantly higher in nonautoreactive CD138$^{int}$ B cells than CD138$^-$ B cells of nonautoimmune mice (Fig. 6), consistent with the observation that some CD138$^{int}$ B cells were IC IgM$^{high}$ and were ASCs (Fig. 4*C*). However, anti-Sm CD138$^{int}$ B cells of nonautoimmune mice, which were not ASCs, did not have elevated Blimp-1 mRNA levels (Fig. 6). Thus, regulation occurred upstream of Blimp-1 transcription. Blimp-1 mRNA levels were significantly elevated in anti-Sm CD138$^{int}$ B cells of MRL/*lpr* mice, and higher still in the anti-Sm CD138$^{high}$ pre-PCs (Fig. 6) consistent with the progressive increase in frequency of cells that were IC IgM$^{high}$ and ASCs. Interestingly, Blimp-1 levels were higher in anti-HEL CD138$^{int}$ B cells than anti-HEL CD138$^-$ B cells. Because the anti-HEL CD138$^{int}$ B cells were not ASCs (data not shown), these data indicate that regulation occurred downstream of Blimp-1 expression. Thus, regulation of autoreactive CD138$^{int}$ B cells can occur before or after Blimp-1 expression.

## Differential BlyS receptor expression in CD138$^{int}$ B cells

BlyS receptors affect the longevity of pre-PCs (35, 36) and thus could influence the life span of anti-Sm CD138$^{int}$ B cells. Using real-time PCR, we determined the relative mRNA expression levels in CD138$^{int}$ and CD138$^-$ B cells of the three BlyS receptors, BAFF-R, TACI, and BCMA. As shown in Fig. 7, CD138$^{int}$ B cells from non-Tg mice had not up-regulated BAFF-R mRNA, but had up-regulated TACI mRNA, a negative regulator of cell survival, and BCMA mRNA, a prosurvival receptor for pre-PCs. Interestingly, the anti-Sm CD138$^{int}$ B cells of 2-12H mice had up-regulated BAFF-R and TACI mRNA, but had not up-regulated BCMA mRNA, while anti-Sm CD138$^{int}$ B cells from MRL/*lpr* mice had up-regulated BAFF-R, TACI, and BCMA mRNAs, and to a much higher level than in nonautoimmune mice. Thus, BCMA mRNA up-regulation correlates with anti-Sm CD138$^{int}$ B cell differentiation to ASCs, suggesting a role for BCMA in their regulation.

## Discussion

In this study, we describe an early pre-PC population of B cells in the BM and spleen of normal mice. They are defined by the expression of intermediate levels of CD138, but normal levels of CD19 and B220. Some are IC $IgM^{high}$ and ASCs. These pre-PCs do not correspond to any other recognized B cell population; based on CD21 and CD23 staining, most resemble FO B cells and some MZ B cells, but the large majority of FO and MZ B cells are $CD138^{-}$. Autoreactive B cells appear to be enriched in this population and a large fraction of them are autoreactive. In nonautoimmune 2-12H mice a large anti-Sm $CD138^{int}$ population is present, but these cells exhibit a more differentiated phenotype than the non-Sm-binding $CD138^{int}$ B cells of non-Tg mice. These data suggest that autoreactive B cells in normal mice have been activated and have begun differentiation toward the PC stage.

A number of findings suggest that the activation of $CD138^{int}$ B cells is Ag driven. This includes the cell surface phenotype and increase in size and granularity relative to $CD138^{-}$ B cells, the lower frequency of $CD138^{int}$ B cells in $CD19^{+/-}$ than $CD19^{+/+}$ mice, and the near absence of anti-HEL $CD138^{int}$ B cells in mice that lack HEL. In addition, the location of $CD138^{int}$ pre-PCs primarily in the follicles proximal to the PALS and bridging channels is suggestive of the B cell migration induced by Ag activation (9). This possible migration is consistent with the chemokine receptor expression changes observed. These data argue that $CD138^{int}$ B cell differentiation is Ag dependent.

The Ags responsible for $CD138^{int}$ B cell differentiation in normal mice are unknown. The analysis of anti-HEL mice and the fact that a large proportion (~20%) of $CD138^{int}$ B cells of non-Tg mice are anti-Sm argues that self-Ags are involved. In fact, the bulk of these cells may be specific for self-Ags and therefore there may be continual pressure to generate $CD138^{int}$ B cells because of the ubiquitous presence of Ag. The distribution of these cells near bridging channels is suggestive of activation by TI Ags, which would be consistent with self-Ag involvement (35). It remains unresolved whether foreign Ags are involved. The autoantibodies produced by these cells may have a normal physiological role and their differentiation to the brink of PC differentiation would ensure a rapid response. Our previous finding that anti-Sm B cells are selected into the MZ and B-1 subsets (30, 31) reinforces the idea of a physiological role for anti-Sm B cells. For the anti-Sm $CD138^{int}$ B cells, the activating Ag may be Sm itself. Sm is exposed on apoptotic cells and immunization with apoptotic cells and soluble Sm induces an anti-Sm response (30). In addition, mice defective in apoptotic cell clearance develop chronically high titers of anti-Sm (30). Thus, the high rate of lymphocyte turnover by apoptosis in the spleen may provide a continuous source of Ag to drive $CD138^{int}$ B cell differentiation.

Important questions regarding the $CD138^{int}$ population in non-Tg mice are yet to be answered. For example, why do $CD138^{int}$ B cells of non-Tg mice and the anti-Sm $CD138^{int}$ B cells of 2-12H mice differ in phenotype (size, granularity, and surface IgM and chemokine receptor expression), and why are there so few $CD138^{high}$ B cells in non-Tg mice, given the large number of $CD138^{int}$ B cells? There are several possible explanations. 1) Many may be autoreactive and regulated to prevent further differentiation. That ~20% of non-Tg $CD138^{int}$ B cells are anti-Sm supports this possibility. 2) They may serve as a reservoir of cells capable of rapid PC differentiation upon encounter with foreign or self-Ags. Along these lines, an interesting possibility is that these cells can move back and forth between the $CD138^{-}$ and $CD138^{int}$ populations. Fujita et al. (37) have demonstrated that the PC transcription program can be reversed and that PCs can reacquire a B cell transcription program and a B cell phenotype. Thus, the $CD138^{-}$ and $CD138^{int}$ populations may exist in dynamic equilibrium controlled by fluctuations in self-Ag concentration. 3) Non-Tg $CD138^{int}$ B cells may in general have low affinity BCRs for their cognate Ag or are exposed

to Ag at concentrations suboptimal for driving differentiation to the CD138$^{high}$ stage. This may result in increased CD138 expression, but not the other changes seen in 2-12H mice. The 2-12H and MD4 × ML5 (anti-HEL/HEL) mice may reveal a more extreme phenotype because of a high affinity of their BCRs for self-Ag. 4) CD138$^{int}$ B cells from non-Tg mice may also exit the spleen and complete their differentiation to PCs elsewhere, although whether these cells can exit the spleen is unknown. CD138$^{int}$ B cells are present in the bone marrow and may derive from splenic B cells, although it cannot be excluded that they arise in situ from newly developed B cells or from recirculating mature CD138$^{-}$ B cells.

The pre-PCs described here appear to precede in differentiation the previously described PC intermediates. PC differentiation involves multiple intermediates whose relationship to each other is ill-defined. There are likely to be multiple pathways for PC differentiation, dictated by several factors, not the least of which is whether the Ag is TI or TD. Several groups have begun to unravel this complexity. Underhill et al. (6), using P- and E-selectin-deficient mice, have proposed a stepwise scheme of PC differentiation. According to this scheme, activated B cells progressively acquire increasing levels of CD138 and decreasing levels of B220 to finally arrive at B220$^{-}$ PCs, which are either CD138$^{int}$ or CD138$^{high}$. Based on this scheme, the CD138$^{int}$ population we have described would likely precede the earliest (CD138$^{high}$) population identified by Underhill et al. (6).

There are also similarities between the CD138$^{int}$ B cells we have described and pre-PCs induced by TD and TI stimulation. Murine mammary tumor virus immunization generates CD138$^{int}$ and CD138$^{high}$ cells (7). They too have up-regulated CXCR4 and down-regulated CXCR5. Likewise, TI stimulation with LPS induces CD138$^{int/high}$ B cells that retain surface IgM. A more comprehensive comparison will be required to understand how these populations are related. Unfortunately, these comparisons provide little insight into the nature of the Ag responsible for the CD138$^{int}$ B cells in unimmunized mice. The CD138$^{int}$ cells in nonautoimmune mice are GL7$^{-}$ (data not shown) and the immunohistochemistry analysis indicates that they are not in germinal centers (Fig. 2), pointing to activation by TI Ags.

Our data demonstrate that the CD138$^{int}$ B cell stage is a checkpoint for the regulation of autoreactive B cells. A higher frequency of CD138$^{int}$ B cells from both non-Tg and 2-12H mice are IC IgM$^{high}$ cells than are their CD138$^{-}$ counterparts, but only the non-Sm binding CD138$^{int}$ B cells become ASCs. The up-regulation of Blimp-1 by non-Sm, but not anti-Sm, CD138$^{int}$ B cells would account for this (12, 13). We also find that these cells have not up-regulated XBP-1 or down-regulated PAX-5 (H. Wang, and S. H. Clarke, manuscript in preparation). The up-regulation of XBP-1 and down-regulation of PAX-5 are important to PC differentiation (15, 38). A CD138$^{int}$ population is present in mice lacking Blimp-1 (14), confirming that Blimp-1 is not required for CD138$^{int}$ B cell differentiation. However, Blimp-1 transcription is up-regulated by anti-HEL B cells (Fig. 5) despite the fact that they do not progress to the ASC stage (data not shown). Thus, a block in PC differentiation can occur at different molecular checkpoints in differentiation. That anti-Sm and anti-HEL B cells differ in this regard suggests that the self-Ag-induced signals control the molecular checkpoint.

Why anti-Sm CD138$^{int}$ B cells fail to up-regulate Blimp-1 is unknown. Bcl-6 represses Blimp-1 transcription, and strong BCR signals can repress Bcl-6, thereby allowing Blimp-1 transcription (39, 40). This model is presented in the context of a germinal center reaction, for which there is no evidence in 2-12H Tg mice, and how Blimp-1 transcription is up-regulated in a TI response is not known. A signal necessary for Blimp-1 transcription, such as a T cell- or DC-derived signal (35, 36), may be lacking, or anti-Sm CD138$^{int}$ B cells may receive a signal that blocks Blimp-1 transcription. For example, anti-Sm pre-PCs may be

susceptible to IL-6-mediated repression by DCs, as described for anergic anti-Sm B cells (41), or to repression by regulatory T cells (42). Alternatively, continuous BCR stimulation may lead to BCR desensitization (43) or sustained ERK phosphorylation (44), either of which might block Blimp-1 transcription. Finally, autoreactive CD138$^{int}$ B cells may be eliminated before Blimp-1 up-regulation, consistent with the rapid turnover rate and high frequency of apoptosis among anti-Sm CD138$^{int}$ B cells in nonautoimmune mice.

The subset origin of CD138$^{int}$ B cells has yet to be determined. The CD23 and CD21 expression by anti-Sm and non-Sm CD138$^{int}$ B cells (Fig. 1*C*) and their location primarily in follicles (Fig. 2) suggests that in nonautoimmune mice most derive from FO B cells. However, because CD23 and CD21 expression levels are altered by activation and MZ B cells migrate toward the PALS upon activation (35), these findings do not exclude or include B cells of any subset as direct precursors. Interestingly, the presence of these cells in MD4 × ML5 mice (Fig. 1*G*) indicates that the same BCR that mediates anergy also mediates CD138$^{int}$ B cell differentiation. One interpretation of this is that anergic B cells can be activated to become CD138$^{int}$ pre-PCs, but a more interesting possibility is that immature or transitional B cells differentiate to either an anergic FO B cell or a CD138$^{int}$ pre-PC depending on the signal they receive. The difference in signal may be the strength of the BCR signal, or the transduction of another signal, such as through a TLR or from DCs (45). The latter hypothesis is attractive because it does not require the activation of anergic B cells.

Comparison of the BlyS receptor expression patterns in Sm- and non-Sm-binding CD138$^{int}$ B cells may provide clues to the regulation of anti-Sm CD138$^{int}$ B cells. BlyS and its receptors BAFF-R, TACI, and BCMA are key players in B cell development and regulation (46) and have different functions (4, 47, 48). They also differ in ability to bind BlyS and the related cytokine a proliferation-inducing ligand (APRIL); BlyS binds all three receptors, while APRIL binds only TACI and BCMA. It is intriguing that BCMA expression is up-regulated by CD138$^{int}$ B cells of non-Tg mice and by anti-Sm CD138$^{int}$ B cells of MRL/*lpr* mice, but not by those of 2-12H Tg mice. Because BCMA is critical for long-term PC survival in part by up-regulating the antiapoptotic gene *Mcl-1* (4), BCMA expression could account for the shortened half-life of anti-Sm CD138$^{int}$ B cells in nonautoimmune mice and survival and continued differentiation in MRL/*lpr* mice.

High TACI levels on anti-Sm CD138$^{int}$ B cells could also contribute to their short half-life. TACI is a negative regulator of BlyS signaling, and TACI-deficient mice develop an SLE-like disease, suggesting that TACI has a role in negative selection of autoreactive B cells (48). To our knowledge, this is the first example of TACI up-regulation by autoreactive B cells. TACI, in the absence of BCMA, may provide a predominantly negative BlyS signal. Although BAFF-R is also up-regulated on anti-Sm CD138$^{int}$ B cells, which could deliver a survival signal (49), non-Tg CD138$^{int}$ B cells have a long half-life in the absence of BAFF-R up-regulation, suggesting that it is not required. Interestingly, APRIL could provide an unopposed negative signal to anti-Sm CD138$^{int}$ B cells, because it binds TACI, but not the BAFF-R. In this model, anti-Sm CD138$^{int}$ B cells of 2-12H MRL/*lpr* mice would receive signals through both TACI and BCMA, which may be sufficient to prolong survival. This speculation highlights the need to understand how BlyS receptor signals are integrated and whether BlyS and APRIL are involved in regulation.

Anti-Sm B cells from MRL/*lpr* mice overcome the CD138$^{int}$ tolerance checkpoint. Many have differentiated to the more PC-like CD138$^{high}$ stage and have become ASCs. The CD138$^{high}$ B cells have lower levels of IgM and other cell surface molecules and increased granularity and size compared with CD138$^{int}$ B cells (Fig. 4). They are similar to late pre-PCs described previously (6, 14). In addition, CD138$^{int}$ and CD138$^{high}$ B cells have

progressively increased Blimp-1 expression and increased XBP-1 expression and decreased PAX-5 expression (Fig. 6 and H. Wang and S. H. Clarke, manuscript in preparation). The immunohistochemistry analysis suggests that CD138$^{int}$ B cells of MRL/*lpr* mice are located predominantly in follicles, as they are in nonautoimmune mice. There is no evidence that they are formed in germinal centers. However, it is possible that many are formed in a TI response, as we speculate for nonautoimmune mice, while a few are activated in a TD response and in germinal centers. The numbers of the cells activated in germinal centers may be too few for detection by the methods used here. Anti-Sm T cells are present in 2-12H MRL/*lpr* mice (50), and thus T cell-derived signals, whether in germinal centers or not, may be involved in driving differentiation of anti-Sm CD138$^{int}$ B cells to become ASCs. Consistent with this, nonautoimmune anti-Sm CD138$^{int}$ B cells can be induced in vitro to become ASCs by anti-CD40 + IL-4 stimulation (data not shown). Other signals may also be important to overcoming tolerance at this checkpoint. Increased levels of serum BlyS have been described in autoimmune NZBWF$_1$ and MRL/*lpr* mice (51), and in SLE patients (52), and thus BlyS could be important to CD138$^{int}$ B cell survival and differentiation due to increased BCMA expression. Increased levels of apoptotic cells (a source of Sm Ag) (53, 54), different cytokine profiles (10), and DC activation could also contribute to overcoming this checkpoint in MRL/*lpr* mice. Fluctuations in any of these factors could affect the rate of ASC differentiation and explain the considerable variability in anti-Sm ASC numbers among CD138$^{int}$ B cells in 2-12 MRL/*lpr* mice. Precisely how the early pre-PC checkpoint is overcome in MRL/*lpr* mice will be an important area for further investigation.

Regulation at an early pre-PC stage prompts new considerations of how B cell tolerance is lost. The anti-Sm CD138$^{int}$ cells in 2-12H mice have been activated and appear to be on the verge of becoming ASCs. The conditions under which these cells can be activated in vivo have yet to be determined. The expression of Blimp-1 and BlyS receptors are potentially critical factors in maintaining these cells at the CD138$^{int}$ stage in normal mice. Thus, there may be an important interface between anti-self BCR stimulation, BlyS/APRIL signaling, and Blimp-1 transcription in determining an appropriate balance between tolerance and activation. Understanding the molecular mechanism of how Blimp-1 and BlyS receptors are regulated in autoreactive B cells may identify new targets for therapeutic intervention in autoimmune diseases.

## Acknowledgments

We gratefully acknowledge the assistance of the Flow Cytometry Facility at the University of North Carolina.

## References

1. Calame KL, Lin KI, Tunyaplin C. Regulatory mechanisms that determine the development and function of plasma cells. Annu. Rev. Immunol. 2003; 21:205–230. [PubMed: 12524387]
2. MacLennan IC, Toellner KM, Cunningham AF, Serre K, Sze DM, Zuniga E, Cook MC, Vinuesa CG. Extrafollicular antibody responses. Immunol. Rev. 2003; 194:8–18. [PubMed: 12846803]
3. O'Connor BP, Gleeson MW, Noelle RJ, Erickson LD. The rise and fall of long-lived humoral immunity: terminal differentiation of plasma cells in health and disease. Immunol. Rev. 2003; 194:61–76. [PubMed: 12846808]
4. O'Connor BP, Raman VS, Erickson LD, Cook WJ, Weaver LK, Ahonen C, Lin LL, Mantchev GT, Bram RJ, Noelle RJ. BCMA is essential for the survival of long-lived bone marrow plasma cells. J. Exp. Med. 2004; 199:91–98. [PubMed: 14707116]
5. Tarte K, Zhan F, De Vos J, Klein B, Shaughnessy J Jr. Gene expression profiling of plasma cells and plasmablasts: toward a better understanding of the late stages of B-cell differentiation. Blood. 2003; 102:592–600. [PubMed: 12663452]

6. Underhill GH, Kolli KP, Kansas GS. Complexity within the plasma cell compartment of mice deficient in both E- and P-selectin: implications for plasma cell differentiation. Blood. 2003; 102:4076–4083. [PubMed: 12881311]
7. Wehrli N, Legler DF, Finke D, Toellner KM, Loetscher P, Baggiolini M, MacLennan IC, Acha-Orbea H. Changing responsiveness to chemokines allows medullary plasmablasts to leave lymph nodes. Eur. J. Immunol. 2001; 31:609–616. [PubMed: 11180126]
8. Hargreaves DC, Hyman PL, Lu TT, Ngo VN, Bidgol A, Suzuki G, Zou YR, Littman DR, Cyster JG. A coordinated change in chemokine responsiveness guides plasma cell movements. J. Exp. Med. 2001; 194:45–56. [PubMed: 11435471]
9. Cyster JG, Ansel KM, Ngo VN, Hargreaves DC, Lu TT. Traffic patterns of B cells and plasma cells. Adv. Exp. Med. Biol. 2002; 512:35–41. [PubMed: 12405185]
10. Cassese G, Arce S, Hauser AE, Lehnert K, Moewes B, Mostarac M, Muehlinghaus G, Szyska M, Radbruch A, Manz RA. Plasma cell survival is mediated by synergistic effects of cytokines and adhesion-dependent signals. J. Immunol. 2003; 171:1684–1690. [PubMed: 12902466]
11. Hauser AE, Debes GF, Arce S, Cassese G, Hamann A, Radbruch A, Manz RA. Chemotactic responsiveness toward ligands for CXCR3 and CXCR4 is regulated on plasma blasts during the time course of a memory immune response. J. Immunol. 2002; 169:1277–1282. [PubMed: 12133949]
12. Lin KI, Tunyaplin C, Calame K. Transcriptional regulatory cascades controlling plasma cell differentiation. Immunol. Rev. 2003; 194:19–28. [PubMed: 12846804]
13. Shaffer AL, Lin KI, Kuo TC, Yu X, Hurt EM, Rosenwald A, Giltnane JM, Yang L, Zhao H, Calame K, Staudt LM. Blimp-1 orchestrates plasma cell differentiation by extinguishing the mature B cell gene expression program. Immunity. 2002; 17:51–62. [PubMed: 12150891]
14. Shapiro-Shelef M, Lin KI, McHeyzer-Williams LJ, Liao J, McHeyzer-Williams MG, Calame K. Blimp-1 is required for the formation of immunoglobulin secreting plasma cells and pre-plasma memory B cells. Immunity. 2003; 19:607–620. [PubMed: 14563324]
15. Iwakoshi NN, Lee AH, Vallabhajosyula P, Otipoby KL, Rajewsky K, Glimcher LH. Plasma cell differentiation and the unfolded protein response intersect at the transcription factor XBP-1. Nat. Immunol. 2003; 4:321–329. [PubMed: 12612580]
16. Angelin-Duclos C, Cattoretti G, Lin KI, Calame K. Commitment of B lymphocytes to a plasma cell fate is associated with Blimp-1 expression in vivo. J. Immunol. 2000; 165:5462–5471. [PubMed: 11067898]
17. Soro PG, Morales AP, Martinez MJ, Morales AS, Copin SG, Marcos MA, Gaspar ML. Differential involvement of the transcription factor Blimp-1 in T cell-independent and -dependent B cell differentiation to plasma cells. J. Immunol. 1999; 163:611–617. [PubMed: 10395648]
18. O'Connor BP, Cascalho M, Noelle RJ. Short-lived and long-lived bone marrow plasma cells are derived from a novel precursor population. J. Exp. Med. 2002; 195:737–745. [PubMed: 11901199]
19. Goodnow CC, Cyster JG, Hartley SB, Bell SE, Cooke MP, Healy JI, Akkaraju S, Rathmell JC, Pogue SL, Shokat KP. Self-tolerance checkpoints in B lymphocyte development. Adv. Immunol. 1995; 59:279–368. [PubMed: 7484462]
20. Gay D, Saunders T, Camper S, Weigert M. Receptor editing: an approach by autoreactive B cells to escape tolerance. J. Exp. Med. 1993; 177:999–1008. [PubMed: 8459227]
21. Nemazee D, Weigert M. Revising B cell receptors. J. Exp. Med. 2000; 191:1813–1817. [PubMed: 10839798]
22. Hartley SB, Crosbie J, Brink R, Kantor AB, Basten A, Goodnow CC. Elimination from peripheral lymphoid tissues of self-reactive B lymphocytes recognizing membrane-bound antigens. Nature. 1991; 353:765–769. [PubMed: 1944535]
23. Lam KP, Rajewsky K. Rapid elimination of mature autoreactive B cells demonstrated by Cre-induced change in B cell antigen receptor specificity in vivo. Proc. Natl. Acad. Sci. USA. 1998; 95:13171–13175. [PubMed: 9789060]
24. Goodnow CC, Crosbie J, Adelstein S, Lavoie TB, Smith-Gill SJ, Brink RA, Pritchard-Briscoe H, Wotherspoon JS, Loblay RH, Raphael K, et al. Altered immunoglobulin expression and functional silencing of self-reactive B lymphocytes in transgenic mice. Nature. 1988; 334:676–682. [PubMed: 3261841]

25. Mandik-Nayak L, Bui A, Noorchashm H, Eaton A, Erikson J. Regulation of anti-double-stranded DNA B cells in nonautoimmune mice: localization to the T-B interface of the splenic follicle. J. Exp. Med. 1997; 186:1257–1267. [PubMed: 9334365]
26. Nguyen KA, Mandik L, Bui A, Kavaler J, Norvell A, Monroe JG, Roark JH, Erikson J. Characterization of anti-single-stranded DNA B cells in a non-autoimmune background. J. Immunol. 1997; 159:2633–2644. [PubMed: 9300682]
27. Roark JH, Bui A, Nguyen KA, Mandik L, Erikson J. Persistence of functionally compromised anti-double-stranded DNA B cells in the periphery of non-autoimmune mice. Int. Immunol. 1997; 9:1615–1626. [PubMed: 9418123]
28. Cyster JG, Hartley SB, Goodnow CC. Competition for follicular niches excludes self-reactive cells from the recirculating B-cell repertoire. Nature. 1994; 371:389–395. [PubMed: 7522305]
29. Santulli-Marotto S, Retter MW, Gee R, Mamula MJ, Clarke SH. Autoreactive B cell regulation: peripheral induction of developmental arrest by lupus-associated autoantigens. Immunity. 1998; 8:209–219. [PubMed: 9492002]
30. Qian Y, Wang H, Clarke SH. Impaired clearance of apoptotic cells induces the activation of autoreactive anti-Sm marginal zone and B-1 B cells. J. Immunol. 2004; 172:625–635. [PubMed: 14688375]
31. Qian Y, Santiago C, Borrero M, Tedder TF, Clarke SH. Lupus-specific antiribonucleoprotein B cell tolerance in nonautoimmune mice is maintained by differentiation to B-1 and governed by B cell receptor signaling thresholds. J. Immunol. 2001; 166:2412–2419. [PubMed: 11160300]
32. Borrero M, Clarke SH. Low-affinity anti-Smith antigen B cells are regulated by anergy as opposed to developmental arrest or differentiation to B-1. J. Immunol. 2002; 168:13–21. [PubMed: 11751941]
33. Santulli-Marotto S, Qian Y, Ferguson S, Clarke SH. Anti-Sm B cell differentiation in Ig transgenic MRL/Mp-lpr/lpr mice: altered differentiation and an accelerated response. J. Immunol. 2001; 166:5292–5299. [PubMed: 11290816]
34. Allman DM, Ferguson SE, Lentz VM, Cancro MP. Peripheral B cell maturation. II. Heat-stable antigen$^{high}$ splenic B cells are an immature developmental intermediate in the production of long-lived marrow-derived B cells. J. Immunol. 1993; 151:4431–4444. [PubMed: 8409411]
35. Martin F, Oliver AM, Kearney JF. Marginal zone and B1 B cells unite in the early response against T-independent blood-borne particulate antigens. Immunity. 2001; 14:617–629. [PubMed: 11371363]
36. Avery DT, Kalled SL, Ellyard JI, Ambrose C, Bixler SA, Thien M, Brink R, Mackay F, Hodgkin PD, Tangye SG. BAFF selectively enhances the survival of plasmablasts generated from human memory B cells. J. Clin. Invest. 2003; 112:286–297. [PubMed: 12865416]
37. Fujita N, Jaye DL, Geigerman C, Akyildiz A, Mooney MR, Boss JM, Wade PA. MTA3 and the Mi-2/NuRD complex regulate cell fate during B lymphocyte differentiation. Cell. 2004; 119:75–86. [PubMed: 15454082]
38. Lin KI, Angelin-Duclos C, Kuo TC, Calame K. Blimp-1-dependent repression of Pax-5 is required for differentiation of B cells to immunoglobulin M-secreting plasma cells. Mol. Cell. Biol. 2002; 22:4771–4780. [PubMed: 12052884]
39. Shaffer AL, Yu X, He Y, Boldrick J, Chan EP, Staudt LM. BCL-6 represses genes that function in lymphocyte differentiation, inflammation, and cell cycle control. Immunity. 2000; 13:199–212. [PubMed: 10981963]
40. Reljic R, Wagner SD, Peakman LJ, Fearon DT. Suppression of signal transducer and activator of transcription 3-dependent B lymphocyte terminal differentiation by BCL-6. J. Exp. Med. 2000; 192:1841–1848. [PubMed: 11120780]
41. Kilmon MA, Rutan JA, Clarke SH, Vilen BJ. Low-affinity, Smith antigen-specific B cells are tolerized by dendritic cells and macrophages. J. Immunol. 2005; 175:37–41. [PubMed: 15972629]
42. Hori S, Takahashi T, Sakaguchi S. Control of autoimmunity by naturally arising regulatory CD4$^{+}$ T cells. Adv. Immunol. 2003; 81:331–371. [PubMed: 14711059]
43. Vilen BJ, Nakamura T, Cambier JC. Antigen-stimulated dissociation of BCR mIg from Ig-α/Ig-β: implications for receptor desensitization. Immunity. 1999; 10:239–248. [PubMed: 10072076]

44. Rui L, Vinuesa CG, Blasioli J, Goodnow CC. Resistance to CpG DNA-induced autoimmunity through tolerogenic B cell antigen receptor ERK signaling. Nat. Immunol. 2003; 4:594–600. [PubMed: 12740574]
45. Leadbetter EA, Rifkin IR, Marshak-Rothstein A. Toll-like receptors and activation of autoreactive B cells. Curr. Dir. Autoimmun. 2003; 6:105–122. [PubMed: 12408049]
46. Zhou T, Zhang J, Carter R, Kimberly R. BLyS and B cell autoimmunity. Curr. Dir. Autoimmun. 2003; 6:21–37. [PubMed: 12408045]
47. Hsu BL, Harless SM, Lindsley RC, Hilbert DM, Cancro MP. Cutting edge: BLyS enables survival of transitional and mature B cells through distinct mediators. J. Immunol. 2002; 168:5993–5996. [PubMed: 12055205]
48. Seshasayee D, Valdez P, Yan M, Dixit VM, Tumas D, Grewal IS. Loss of TACI causes fatal lymphoproliferation and autoimmunity, establishing TACI as an inhibitory BLyS receptor. Immunity. 2003; 18:279–288. [PubMed: 12594954]
49. Cancro MP, Smith SH. Peripheral B cell selection and homeostasis. Immunol. Res. 2003; 27:141–148. [PubMed: 12857963]
50. Yan J, Mamula MJ. Autoreactive T cells revealed in the normal repertoire: escape from negative selection and peripheral tolerance. J. Immunol. 2002; 168:3188–3194. [PubMed: 11907071]
51. Gross JA, Johnston J, Mudri S, Enselman R, Dillon SR, Madden K, Xu W, Parrish-Novak J, Foster D, Lofton-Day C, et al. TACI and BCMA are receptors for a TNF homologue implicated in B-cell autoimmune disease. Nature. 2000; 404:995–999. [PubMed: 10801128]
52. Roschke V, Sosnovtseva S, Ward CD, Hong JS, Smith R, Albert V, Stohl W, Baker KP, Ullrich S, Nardelli B, et al. BLyS and APRIL form biologically active heterotrimers that are expressed in patients with systemic immune-based rheumatic diseases. J. Immunol. 2002; 169:4314–4321. [PubMed: 12370363]
53. Casciola-Rosen LA, Anhalt G, Rosen A. Autoantigens targeted in systemic lupus erythematosus are clustered in two populations of surface structures on apoptotic keratinocytes. J. Exp. Med. 1994; 179:1317–1330. [PubMed: 7511686]
54. Rosen A, Casciola-Rosen L. Autoantigens as substrates for apoptotic proteases: implications for the pathogenesis of systemic autoimmune disease. Cell Death Differ. 1999; 6:6–12. [PubMed: 10200542]

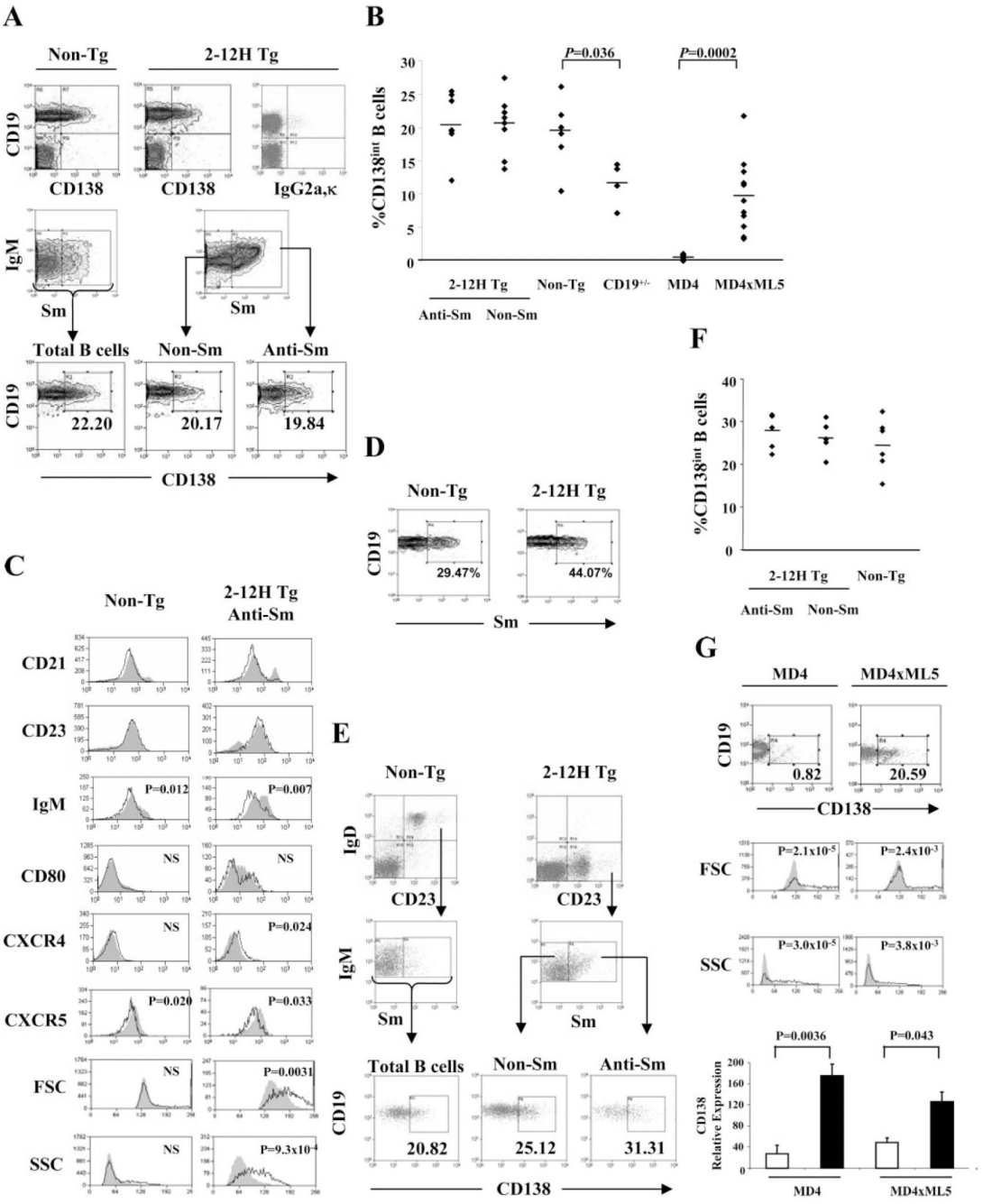


**FIGURE 1.**

$CD138^{int}$ cells are present at a high frequency in the spleens and BM of non-Tg and 2-12H mice. *A*, CD138 expression by splenic B cells. *Top row*, CD19 and CD138 staining of total splenic lymphocytes in non-Tg and 2-12H littermates as determined by forward scatter (FSC) and side scatter (SSC). The *right histogram* is a representative isotype (IgG2a,κ) control stain (1.19 ± 0.25% ($n$ = 4) falling within the $CD19^+$, $CD138^+$ quadrant). *Middle row*, Shown are histograms for IgM and Sm staining of $CD19^+$ B cells from non-Tg and 2-12H mice. The indicated gate is that for the $Sm^+$ population analyzed in the *bottom row. Bottom row*, Shown is the CD138 expression of gated $Sm^+$ and $Sm^-$ B cells from 2-12H mice and total B cells from non-Tg mice. The percentage of $CD19^+$ B cells that are

CD138$^{int}$ is provided. *B*, Frequency of CD19$^{+}$CD138$^{int}$ B cells among CD19$^{+}$ B cells. Each symbol represents a single mouse and a horizontal line marks the mean. Absolute numbers of CD138$^{int}$ B cells are $5.48 \times 10^6 \pm 1.16 \times 10^6$ ($n = 8$) for 2-12H anti-Sm, $8.19 \times 10^6 \pm 1.77 \times 10^6$ ($n = 8$) for 2-12H non-Sm, and $2.37 \times 10^7 \pm 6.47 \times 10^6$ ($n = 6$) for non-Tg mice, $4.91 \times 10^6 \pm$ (*Figure legend continues*) $4.66 \times 10^5$ ($n = 4$) for CD19$^{+/-}$ mice, $2.7 \times 10^5 \pm 1.63 \times 10^5$ ($n = 8$) in MD4 mice, and $1.20 \times 10^6 \pm 4.76 \times 10^5$ ($n = 11$) in MD4 × ML5 mice. *C*, Activation marker expression by CD19$^{+}$ CD138$^{-}$ B cells (shaded) and CD19$^{+}$ CD138$^{int}$ (black line) from non-Tg and 2-12H mice. Representative histograms are shown. Values of *p* are given for the differences between the CD138$^{int}$ and CD138$^{-}$ cells. *D*, Sm binding by CD138$^{int}$ B cells. Histograms are gated on CD138$^{int}$ B cells from the indicated mice as illustrated in *A* (*upper right quadrant* of *top row*). The percentage of anti-Sm CD138$^{int}$ B cells is provided. The average percentage for non-Tg and 2-12H mice is given in Table I. *E*, CD138 expression by BM B cells. *Top row*, Histograms are gated on CD19$^{+}$ cells to identify the recirculating IgD$^{+}$CD23$^{+}$ B cells. *Middle row*, Sm binding by gated IgD$^{+}$ CD23$^{+}$ B cells. *Bottom row*, CD138 expression by the indicated B cell subsets. The percentage of gated B cells that are CD138$^{+}$ is given. *F*, Frequency of CD138$^{int}$ B cells among the recirculating IgD$^{+}$CD23$^{+}$ B cells of the BM. Each symbol represents a single mouse and a horizontal line marks the mean. *G*, CD19$^{+}$ CD138$^{int}$ B cells are absent in anti-HEL MD4 mice, but present in anti-HEL/HEL MD4 × ML5 mice. Frequency of CD138$^{int}$ B cells is given as percent of CD19$^{+}$ B cells. The FSC and SSC for CD138$^{-}$ (shaded) and CD138$^{int}$ (solid line) B cells are shown along with the *p* values for the differences in mean fluorescence intensities. The gating for CD138$^{int}$ cells is indicated in the *top histograms*. The CD138$^{-}$ B cells were all CD19$^{+}$ cells that fell outside the CD138$^{int}$ gate. *Lower graph* shows real-time PCR results for CD138 expression using sorted CD138$^{-}$ and CD138$^{int}$ B cells from MD4 and MD4 × ML5 mice.

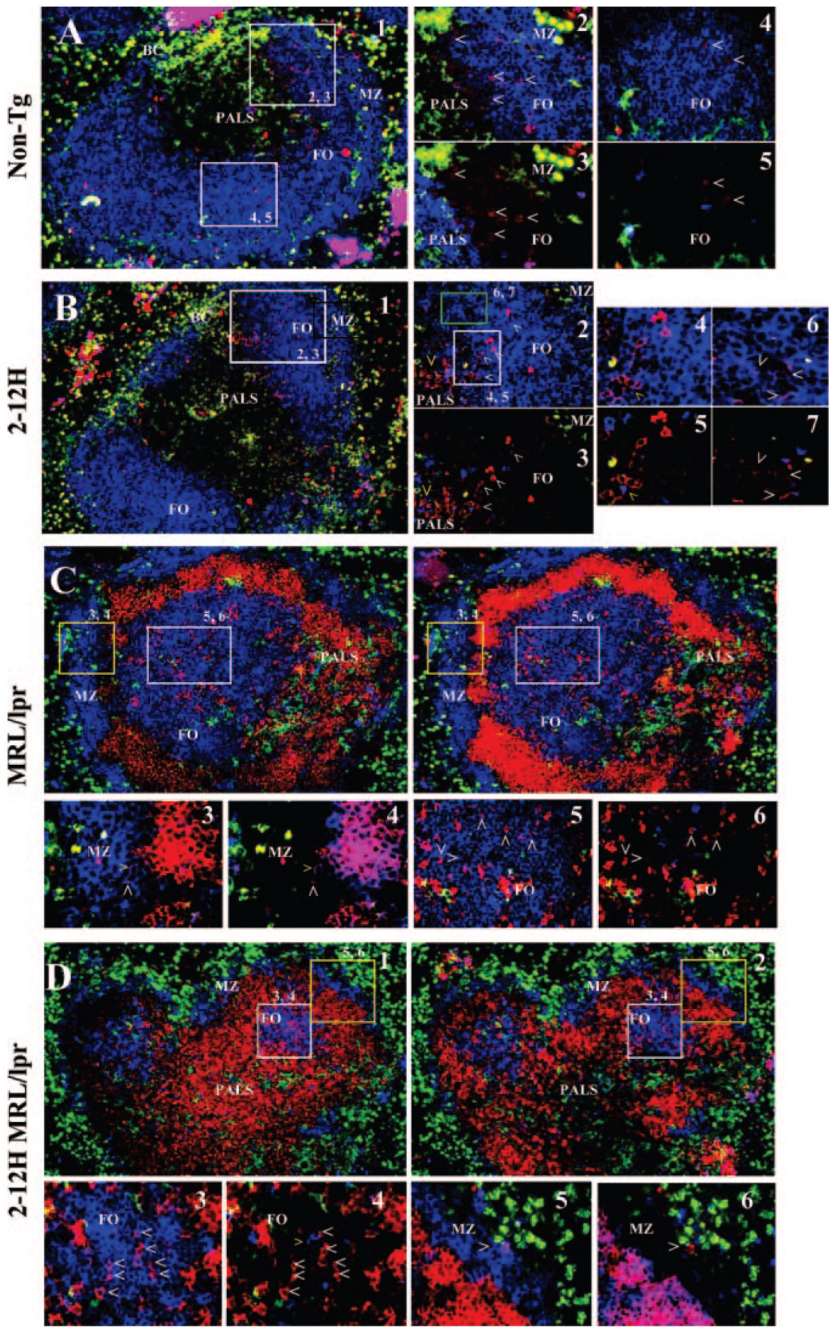


**FIGURE 2.**

Immunofluorescence analysis of nonautoimmune and autoimmune mice. Spleens were sectioned and stained with anti-CD138 and anti-IgM, anti-CD3, anti-CD11b, and anti-CD11c to identify B cells, T cells, macrophages, and DCs, respectively. *A,* Non-Tg: A representative follicle at ×10 magnification is shown in *panel 1*. B cells are blue, CD138 is red, and macrophages/DCs are green. The locations and corresponding photos for the higher magnifications (×40) are indicated. *Panels 2* and *4* are stained identically to A1, but in *panels 3* and *5*, T cells are blue and B cells are not shown. White carets identify examples of $CD138^{+}$ B cells. *Panels 2* and *3* show a clustering of $CD138^{int}$ B cells near a bridging channel (BC). Note that the $CD138^{+}$ B cells are more frequent near the PALS and bridging

channel. *Panels 4* and *5* show an area of the follicle away from the bridging channel in which $CD138^+$ B cells are infrequent. *B*, 2-12H: *Panels 1–3* are as described for the corresponding photos in *A*. *Panels 4–6* are higher magnification (×64) of the indicated areas indicated in *panel 2*. *Panels 4* and *6* show B cells (blue), but not T cells; *panels 5* and *7* show T cells (blue), but not B cells. *Panels 2–6* show an area near a bridging channel. Note the greater concentration of $CD138^+$ B cells near the PALS and bridging channel. White carets identify representative $CD138^+$ B cells. The yellow carrot shows an example of a T cell near a cluster of $CD138^+$ B cells. *C*, MRL/*lpr*: *Panels 1* and *2* show a representative follicle at ×10 magnification. *Panel 1* shows B cells (blue), macrophages/DCs (green), and T cells (red). In this view, T cells have infiltrated into the marginal sinus. *Panel 2* shows the same follicle with B cells (blue), macrophages/DCs (green), and CD138 (red). Note that many T cells are $CD138^+$. *Panels 3* and *4* show the MZ area (×40 magnification), and *panels 5* and *6* show a follicle (×40 magnification). *Panels 3* and *5* show B cells (blue) but not T cells; *panels 4* and *6* show T cells (blue), but not B cells. *D,* 2-12H MRL/*lpr*. Same as *C. Panels 3* and *4* show the follicle; *panels 5* and *6* show the MZ.

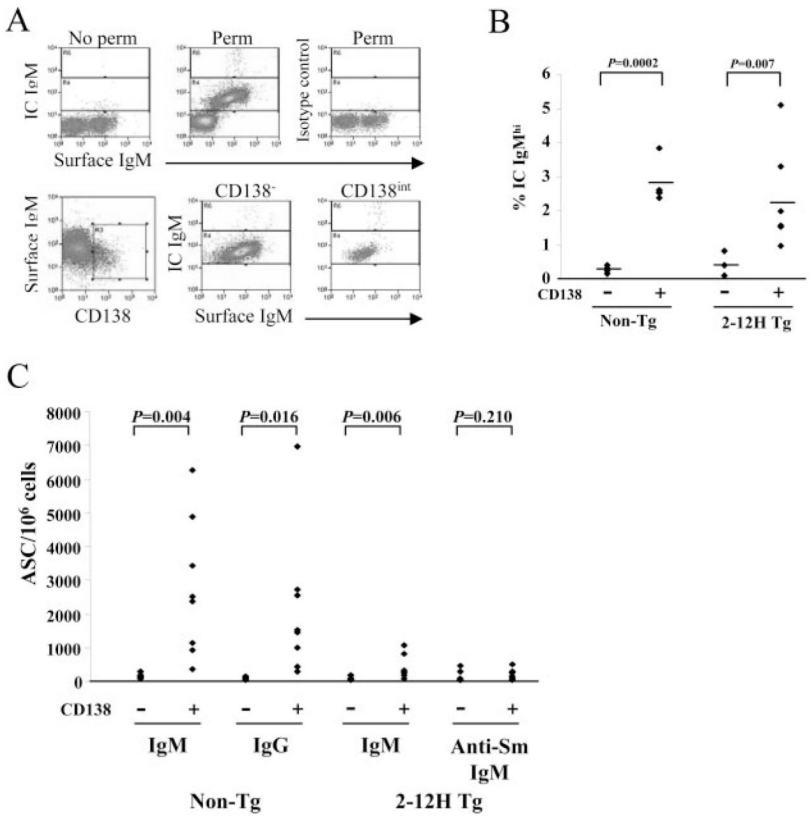


**FIGURE 3.**

A subset of CD138$^{int}$ B cells are IC Ig-M$^{high}$ and secrete Ab, but anti-Sm CD138$^{int}$ B cells do not secrete Ab. *A*, Surface and IC IgM on non-Tg CD138$^{-}$ and CD138$^{int}$ B cells. Nonpermeabilized and isotype controls do not show IC IgM staining (*top row*). CD138$^{-}$ and CD138$^{int}$ B cells were gated as indicated (*bottom row*; *left histogram*) and the percentage of IC IgM$^{+}$ B cells that are IC IgM$^{high}$ determined (*second row*; *middle* and *right histograms*) and displayed in *B*. The *bottom* and *top gates* indicate the IC IgM$^{low}$ and IC IgM$^{high}$ populations, respectively. *B*, The frequency of IC IgM$^{high}$ cells among CD138$^{-}$ and CD138$^{int}$ B cells from non-Tg and 2-12H mice. The horizontal line marks the mean frequency. *C*, The number of ASCs per $10^6$ sorted CD138$^{-}$ or CD138$^{int}$ B cells detected by ELIS-POT. IgM and IgG ELISPOT assays were used for analysis of non-Tg mice, and IgM and anti-Sm ELISPOT assays were used for analysis of 2-12H mice. The total number of ASCs per spleen is presented in Table II.

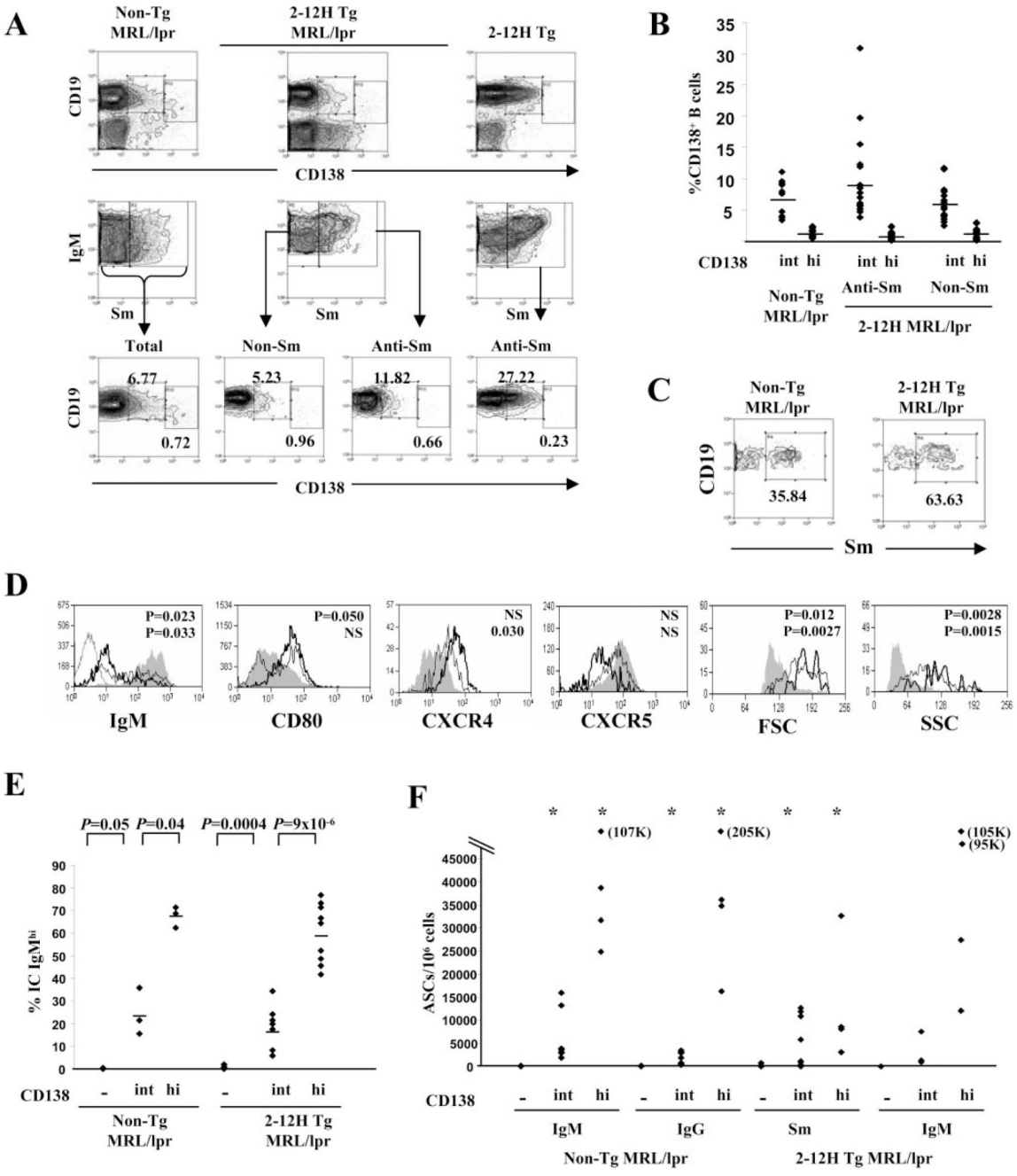


**FIGURE 4.**

Anti-Sm CD138$^{int}$ B cells are ASCs in autoimmune mice. *A*, CD19$^{+}$CD138$^{int}$ and CD19$^{+}$CD138$^{high}$ B cells are present in non-Tg MRL/*lpr* mice and as anti-Sm and non-Sm B cells in 2-12H MRL/*lpr* mice. T cells from MRL/*lpr* mice express CD138 and have been excluded from the histograms of the *top row* by anti-CD3 staining and gating on the CD3-negative cells. The histograms of the *middle row* are gated on CD19$^{+}$ lymphocytes, and the *bottom row* on the indicated Sm-binding or non-Sm-binding populations. *B*, Frequency of CD19$^{+}$CD138$^{int}$ and CD19$^{low}$CD138$^{high}$ B cells as a percentage of CD19$^{+}$ B cells. Each symbol represents a single mouse, and the horizontal line marks the mean frequency. The number of CD19$^{+}$CD138$^{int}$ B cells is as follows: $9.48 \times 10^{6} \pm 3.55 \times 10^{6}$ for non-Tg MRL/

*lpr* (frequency: 6.8 ± 2.5% of $CD19^+$ B cells); $2.12 \times 10^6 \pm 1.49 \times 10^6$ for 2-12H MRL/*lpr* anti-Sm (frequency: 3.0 ± 2.1% of $CD19^+$ B cells); and $2.67 \times 10^6 \pm 1.31 \times 10^6$ for 2-12H MRL/*lpr* non-Sm (frequency: 3.8 ± 1.8% of $CD19^+$ B cells). The number of $CD19^{low}CD138^{high}$ cells are as follows: $1.46 \times 10^6 \pm 8.46 \times 10^5$ for non-Tg MRL/*lpr* (frequency: 1.04 ± 0.174% of $CD19^+$ B cells); $1.48 \times 10^5 \pm 1.20 \times 10^5$ for 2-12H MRL/*lpr* anti-Sm (frequency: 0.66 ± 0.130% of $CD19^+$ B cells); and $4.27 \times 10^5 \pm 3.52 \times 10^5$ for 2-12H MRL/*lpr* non-Sm (frequency: 0.900 ± 0.180% of $CD19^+$ B cells). The number and frequency of $CD138^{int}$ from 2-12H nonautoimmune mice is given in Fig. 1. The number of anti-Sm $CD138^{high}$ B cells in 2-12H mice is $4.24 \times 10^4 \pm 8.33 \times 10^3$ (frequency: 0.127 ± 0.0249% of $CD19^+$ B cells). The number of $CD138^{high}$ B cells in nonautoimmune non-Tg mice is $2.92 \times 10^5 \pm 5.78 \times 10^4$ (frequency: 0.23 ± 0.047% of $CD19^+$ B cells) (using gates (*Figure legend continues*) identical to those used for 2-12H mice). The frequency of anti-Sm $CD138^{high}$ B cells in 2-12H and 2-12H MRL/*lpr* mice differs significantly ($p = 0.0084$). *C*, Sm binding by $CD138^{int}$ B cells. Histograms are gated on $CD138^{int}$ B cells from the indicated mice as illustrated in *A* (*upper right quadrant* of *top row*). The percentage of anti-Sm $CD138^{int}$ B cells is provided. The average percentage for non-Tg and 2-12H mice is given in Table I. *D*, FSC, SSC, and activation marker expression for $CD19^+CD138^-$ (shaded), $CD19^+CD138^{int}$ (thin black line), and $CD19^{low}CD138^{high}$ (thick black line) B cells from 2-12H Tg MRL/*lpr* mice. Representative histograms are shown. Anti-IgM levels on T cells are shown as a negative control for IgM expression in the *first panel*. The *p* values for the differences between $CD138^-$ and $CD138^{int}$ (*top value*) and between $CD138^{int}$ and $CD138^{high}$ (*bottom value*) are given. *E*, The frequency of IC $IgM^{high}$ cells among $CD138^-$, $CD138^{int}$, and $CD138^{high}$ B cells from non-Tg and 2-12H Tg MRL/*lpr* mice. The horizontal line marks the mean frequency. The *p* values for the relevant comparisons are shown. *F*, ASCs among $10^6$ sorted $CD138^-$, $CD138^{int}$, and $CD138^{high}$ B cells from non-Tg MRL/*lpr* and 2-12H MRL/*lpr* mice. *, Statistical significance from $CD138^-$ B cells ($p < 0.05$). The ELISPOT assays were as described for Fig. 1. Note that the scale is different from that for Fig. 3*C*.

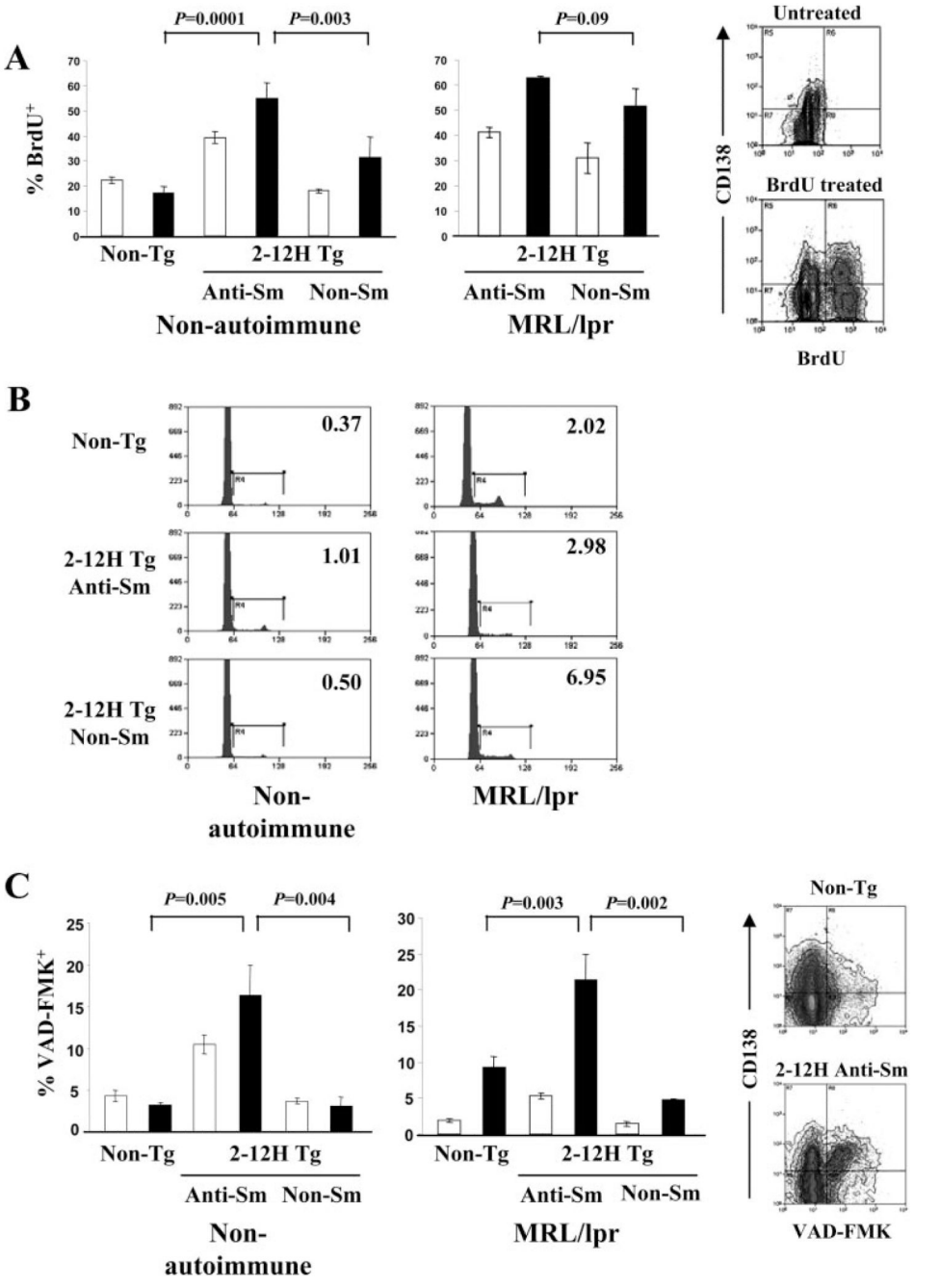


**FIGURE 5.**

Anti-Sm CD138$^{int}$ B cells have a high turnover rate and a high frequency are undergoing apoptosis. *A*, Seven-day BrdU incorporation by CD138$^{-}$ (□) and CD138$^{int}$ (■) B cells from non-Tg, 2-12H, and 2-12H MRL/*lpr* mice ($n = 4$). Error bars indicate SD. On the *right* are representative histograms to illustrate the gatings used to measure the frequency CD138$^{-}$ and CD138$^{int}$ populations that have incorporated BrdU. *B*, Cell cycle analysis of CD138$^{int}$ B cells based on propidium iodide (PI) incorporation. The frequency of PI$^{+}$ cells in the $G_2$/S gate is shown for each population. Representative of two independent experiments using cells pooled from three mice. *C*, Detection of early apoptosis using VAD-FMK staining of CD138$^{-}$ (□) and CD138$^{int}$ (■) B cells in non-Tg, 2-12H, and 2-12H MRL/*lpr* mice ($n = 6$).

Error bars indicate SD. On the *right* are representative histograms illustrating the gates for VAD-FMK and CD138 staining used to generate the frequency of apoptotic cells. Values of *p* are for the comparison between the indicated $CD138^{int}$ populations.

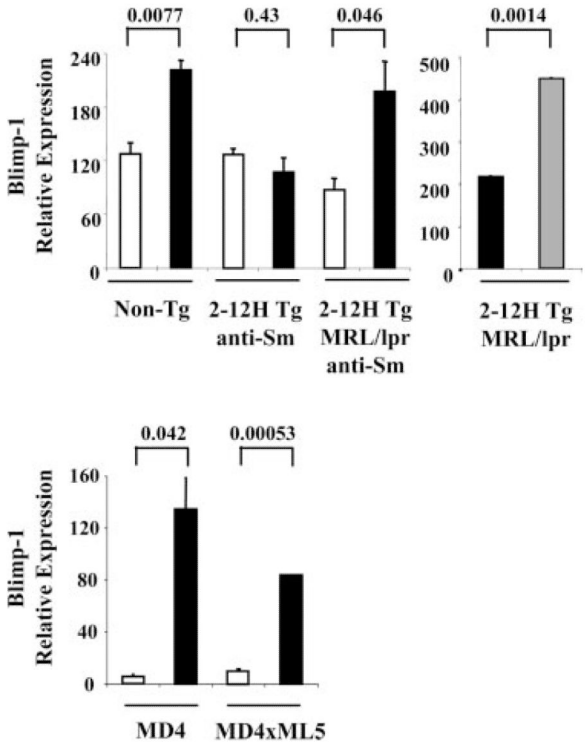


**FIGURE 6.**

Blimp-1 mRNA is up-regulated in CD138$^{int}$ B cells that secrete Ab. Shown are Blimp-1 mRNA levels from sorted CD138$^{-}$ (□) and CD138$^{int}$ (■) B cells from non-Tg mice and sorted anti-Sm CD138$^{-}$ and CD138$^{int}$ B cells from 2-12H and 2-12H MRL/*lpr* mice. The *right panel* shows Blimp-1 mRNA levels in CD138$^{int}$ (■) and CD138$^{high}$ (▩) B cells in 2-12H MRL/*lpr*. In the *lower graph* are relative Blimp-1 levels from sorted CD138$^{-}$ and CD138$^{int}$ B cells from MD4 and MD4 × ML5 mice. Data are representative of two independent experiments using pooled mice. Values of *p* are shown for the indicated comparisons.

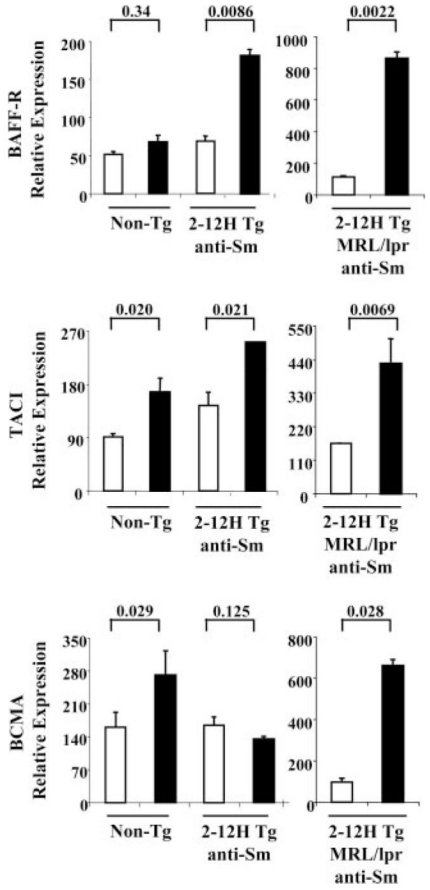


**FIGURE 7.**

Differential expression of BAFF-R, TACI, and BCMA on anti-Sm and non-Tg CD138$^{int}$ B cells. BAFF-R, TACI, and BCMA mRNA levels in CD138$^{-}$ (□) and CD138$^{int}$ (■) non-Tg B cells and anti-Sm B cells from 2-12H and 2-12H MRL/*lpr* mice. Data are representative of two independent experiments using pooled mice. Values of *p* are shown for the indicated comparisons.

## Table I

### Fraction of CD138$^{int}$ and CD138$^{neg}$ B cells that were anti-Sm[a]

| | CD138$^{int}$ | CD138$^{neg}$ |
|---|---|---|
| Non-Tg ($n$ = 7) | 21.5 ± 6.56 | 12.9 ± 3.44[b] |
| 2-12H ($n$ = 9) | 49.8 ± 4.87[c] | 47.9 ± 4.56[c] |
| MRL/*lpr* ($n$ = 4) | 34.2 ± 9.02 | 11.0 ± 5.07[b] |
| 2-12H MRL/*lpr* ($n$ = 7) | 52.4 ± 9.02[c] | 24.5 ± 5.52[b,c] |

[a] The percentage of anti-Sm B cells within the indicated population ± SE.

[b] A significant difference ($p < 0.01$) between CD138$^{int}$ and CD138$^{neg}$ of the same mouse strain.

[c] A significant difference ($p < 0.01$) between 2–12H and non-Tg mice or between MRL/*lpr* and 2-12H MRL/*lpr* mice.

**Table II**

**ASCs secreting IgM, IgG, or anti-Sm per spleen in nonautoimmune and autoimmune mice (×10$^3$)**

| | Non-Tg | | 2-12H | | Non-Tg MRL/*lpr* | | | 2-12H MRL/*lpr* | | |
|---|---|---|---|---|---|---|---|---|---|---|
| | **CD138$^-$** | **CD138$^{int}$** | **CD138$^-$** | **CD138$^{int}$** | **CD138$^-$** | **CD138$^{int}$** | **CD138$^{high}$** | **CD138$^-$** | **CD138$^{int}$** | **CD138$^{high}$** |
| IgM | 8.43 ± 2.43[a] (8) | 64.0 ± 1.71[b] (8) | 2.38 ± 2.00 (8) | 6.34 ± 1.96[c] (8) | 11.3 ± 2.37 (8) | 56.8 ± 18.1[c] (8) | 73.9 ± 27.9[d] (4) | 3.68 ± 0.919 (11) | 13.7 ± 7.69 (11) | 34.3 ± 13.4 (4) |
| IgG | 5.98 ± 1.22 (8) | 49.3 ± 1.81[c] (8) | ND | ND | 6.07 ± 2.08 (8) | 17.7 ± 4.13[c] (8) | 106 ± 64.5[ce] (4) | ND | ND | ND |
| Anti-Sm | ND | ND | 9.63 ± 6.24 (8) | 2.13 ± 0.739 (8) | ND | ND | ND | 8.23 ± 4.70 (4) | 19.8 ± 7.46 (4) | 7.53 ± 3.80 (4) |

[a] Average ± SE; the number of mice analyzed for each value is provided in parentheses.

[b] $p < 0.01$

[c] $p < 0.05$, between CD138$^-$ and CD138$^{int}$ cells, or between CD138$^{int}$ and CD138$^{hgh}$ cells.

[d] $p < 0.01$

[e] $p < 0.05$, between CD138$^-$ and CD138$^{high}$ cells.